STEM CELLS AND DEVELOPMENT
Volume 28, Number 4, 2019

DOI: 10.1089/scd.2018.0197

Remodeling of Glycosaminoglycans During Differentiation of Adult Human Bone Mesenchymal Stromal Cells Toward Hepatocytes

Paiyz E. Mikael,[1] Charles Willard,[2] Aurvan Koyee,[3] Charmaine-Grace Barlao,[4] Xinyue Liu,[1,2,5] Xiaorui Han,[1,5] Yilan Ouyang,[1] Ke Xia,[1] Robert J. Linhardt,[1,2,4,5] and Jonathan S. Dordick[1,2,4,5]

There is a critical need to generate functional hepatocytes to aid in liver repair and regeneration upon availability of a renewable, and potentially personalized, source of human hepatocytes (hHEP). Currently, the vast majority of primary hHEP are obtained from human tissue through cadavers. Recent advances in stem cell differentiation have opened up the possibility to obtain fully functional hepatocytes from embryonic or induced pluripotent stem cells, or adult stem cells. With respect to the latter, human bone marrow mesenchymal stromal cells (hBMSCs) can serve as a source of autogenetic and allogenic multipotent stem cells for liver repair and regeneration. A major aspect of hBMSC differentiation is the extracellular matrix (ECM) composition and, in particular, the role of glycosaminoglycans (GAGs) in the differentiation process. In this study, we examine the influence of four distinct culture conditions/protocols (T1–T4) on GAG composition and hepatic markers. α-Fetoprotein and hepatocyte nuclear factor-4α were expressed continually over 21 days of differentiation, as indicated by real time quantitative PCR analysis, while albumin (ALB) expression did not begin until day 21. Hepatocyte growth factor (HGF) appears to be more effective than activin A in promoting hepatic-like cells through the mesenchymal–epithelial transition, perhaps due to the former binding to the HGF receptor to form a unique complex that diversifies the biological functions of HGF. Of the four protocols tested, uniform hepatocyte-like morphological changes, ALB secretion, and glycogen storage were found to be highest with protocol T2, which involves both early- and late-stage combinations of growth factors. The total GAG profile of the hBMSC ECM is rich in heparan sulfate (HS) and hyaluronan, both of which fluctuate during differentiation. The GAG profile of primary hHEP showed an HS-rich ECM, and thus, it may be possible to guide hBMSC differentiation to more mature hepatocytes by controlling the GAG profile expressed by differentiating cells.

Keywords: adult mesenchymal stromal cells, GAG temporal remodeling, heparan sulfate, chondroitin sulfate, hyaluronan, functional hepatocytes

Introduction

Primary human hepatocytes (hHEP) are rapidly becoming indispensable in drug discovery, human toxicology, and regenerative medicine [1]. These cells are typically obtained from deceased individuals and then cryopreserved for subsequent use; however, they quickly lose phenotypic properties upon culturing, which limits their use [2]. Recent advances in human embryonic stem cells (hESCs) and human induced pluripotent stem cells (hiPSCs) may ultimately obviate the need to obtain fresh hepatocytes from human donors. hESCs and induced pluripotent stem cells are able to commit to an endodermal lineage, which can be terminally differentiated into hepatocytes [3–5]. However, differentiating hESCs or hiPSCs into functional hepatocytes remains difficult with variable degrees of functionality achieved and with low yield [6,7].

Recently, adult mesenchymal stromal cells derived from bone marrow (BMSCs), and stromal stem cells (MSCs) from more readily available tissues, such adipose and umbilical cord, have been investigated as potential hepatocyte sources. However, relatively little work has been performed in using these adult cells outside of examples with rodents [8–10]. In particular, methods of differentiating human BMSCs (hBMSCs) and hMSCs into hepatocytes are not sufficiently advanced. To that end, work to date has focused

[1]Center for Biotechnology and Interdisciplinary Studies, [2]Department of Chemical and Biological Engineering, [4]Department of Biochemistry and Biophysics, and [5]Department of Chemistry and Chemical Biology, Rensselaer Polytechnic Institute, Troy, New York.
[3]Department of Biology, University of Virginia, Charlottesville, Virginia.

on exogenous chemical and physical cues, such as extracellular matrix (ECM) composition, biomaterial stiffness and cell morphology [11–13], and static versus dynamic culturing [8].

It is well established that the local ECM plays a major role in cell fate and function [14], and a major component of the ECM is the glycosaminoglycans (GAGs). Unfortunately, little work has been undertaken to understand the influence of GAG composition and changes to GAG composition on stromal cell differentiation. In previous work, we showed that dramatic changes to GAG type and composition in hESCs occur as the cells differentiate into early mesoderm and endoderm lineages [15]. Separately, highly sensitive liquid chromatography–tandem mass spectrometry (LC-MS/MS) was used to detect very low amounts of GAGs in tissue samples and cells, which resulted in new insights into the temporal remodeling of GAG type and composition in hESC differentiation [16].

Based on these previous studies, we hypothesize that methods to control GAG type and composition, effectively the ''GAGome,'' can be used to optimize hBMSC differentiation into complex terminal cell types, such as primary hHEP. In this work, we show that, although all four protocols (T1–T4) could direct differentiation of hBMSCs toward a hepatic lineage, one protocol (T2) stood out in terms of morphology and functional performance. While none of the protocols produced mature hepatocytes, by identifying the profile changes of GAGs and their component disaccharides, it may be possible to further optimize differentiation and maturation based on controlling GAG profiles during differentiation.

Materials and Methods

Isolation and culture of adult hBMSCs

Ten milliliters of unprocessed fresh bone marrow was purchased from Lonza (Walkersville, MD). Bone marrow was diluted to 5–10 million cells/mL in Dulbecco's modified Eagle medium and Ham's F12 with Glutamax (DMEM/F12; Life Technologies). Cells were then layered over Ficoll-Paque and centrifuged at $450 \times g$ for 40 min at room temperature. The mononuclear cell fraction was collected and resuspended in growth media, seeded onto 75 cm^2 culture flasks, and cultured at 37°C in humidified atmosphere containing 5% CO_2. Growth media consisted of DMEM/F12 with Glutamax, 10% fetal bovine serum (FBS; Life Technologies), and 1% penicillin–streptomycin (Life Technologies). Nonadherent cells were removed after 4 days by gently washing with phosphate-buffered saline (PBS; Invitrogen). The culture medium was changed every 3 days and cells were passaged at ~90% confluence. All experiments were performed at passage 3 or 4. Cryoplateable primary hHEP were cultured according to the manufacturer's protocol (Millipore-Sigma).

Hepatic differentiation protocols

Four protocols were compared to identify the differentiation conditions that produced functional hepatocyte-like cells (Fig. 1). In all differentiation protocols, DMEM/F12 medium without FBS was used, a sequential two-step method (differentiation and maturation) was employed, and the protocols were divided into two groups. The first group (protocols T1A, B, and C) consisted of a mesoderm-to-endoderm (MET) initiation step where hBMSCs are first induced by the addition of 25, 50, or 100 ng/mL of activin A (R&D Systems), respectively, with 10 ng/mL epithelial growth factor (EGF; Thermo Fisher Scientific) and beta-fibroblast growth factor (bFGF; Fisher Scientific). The differentiation step included 50 ng/mL hepatocyte growth factor (HGF; Thermo Fisher Scientific), 30 ng/mL bFGF, 20 ng/mL EGF, 1× Premix culture supplement (100× stock; Millipore-Sigma), and 0.6 mg/mL nicotinamide (Sigma). For the maturation step, 20 ng/mL oncostatin M (OSM; Fisher Scientific), 1 μM dexamethasone (Sigma), and 0.1% dimethyl sulfoxide (DMSO) were added. The second group (protocols T2, T3, and T4) included direct differentiation without an EMT initiation step. T2 differentiation included 20 ng/mL HGF, 10 ng/mL bFGF, and 0.61 g/L nicotinamide followed by maturation with 20 ng/mL OSM, 50 mg/mL ITS+, and 1 μM dexamethasone. T3 differentiation included 20 ng/mL HGF, 100 μM dexamethasone, and 50 mg/mL ITS+ followed by maturation with 20 ng/mL OSM, 100 mM dexamethasone, and 50 mg/mL ITS+. T4 differentiation was performed in two stages; stage one included 10 ng/mL each of fibroblast growth factor-4 (FGF-4; PeproTech) and ITS+. Stage two included 20 ng/mL HGF, which continued into maturation by addition of 1× ITS+ and 1 μg/mL dexamethasone. Undifferentiated hBMSCs were cultured in DMEM/F12 medium with 10% FBS.

Quantitative real time-quantitative polymerase chain reaction

Key early and mature hepatic markers were evaluated in differentiated and nondifferentiated hBMSCs, and primary hepatocytes, all cultured in 24-well plates. At predetermined time points, cells were washed with PBS, and the total RNA was isolated using Direct-zol (Zymo Research) following the manufacturer's protocol. After isolation, 0.1–1.0 μg of RNA was converted to cDNA and amplified using the high capacity reverse transcription kit (Invitrogen). Real-time quantitative polymerase chain reaction (qPCR) was performed using TaqMan gene expression master mix (ThermoFisher). The threshold cycle values of target genes were standardized against human glyceraldehyde 3-phosphate dehydrogenase (GAPDH) (Hs02758991) expression. Genes for human AFP (α-fetoprotein; Hs00173490), human hepatocyte nuclear factor (HNF)-4α (Hs00230853), and human albumin (ALB) (Hs00609411) were quantified and normalized to the housekeeping gene, GAPDH. Relative expression fold changes were determined by normalizing to those of undifferentiated hBMSCs.

Periodic acid and Schiff's solution staining

At the end of hBMSC maturation (day 21), intracellular glycogen was analyzed (Periodic Acid-Schiff [PAS] staining system; Sigma). Cells, plated in 24-wells, were fixed in a 10% formaldehyde solution for 10 min and then rinsed in distilled deionized (DDI) water. Following the manufacturer's protocol, cells were stained with a periodic acid solution. After rinsing with DDI water, cells were immersed in Schiff's reagent for 15 min tand hen washed with DDI water for 5 min. Samples were counterstained for the nucleus with hematoxylin for 90 s and then washed in running water for 30 s. Samples were air dried and imaged.

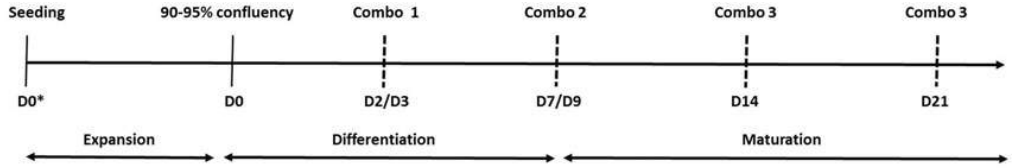

Treatment	Differentiation		Maturation	Reference
T1A, B, C	Day 0-1: MET Initiation 20, 50 or 100ng/ml AA 10ng/ml EGF 10ng/ml bFGF	Day 2-9: 50ng/ml HGF 30ng/ml bFGF 20ng/ml EGF 1X ITS$^+$ 0.6mg/ml Nicotinamide	Day 10-21: 20ng/ml OSM 1uM Dexamthasone 0.1% DMSO	SW Lee et al.
T2	Day 0-6: 20ng/ml HGF 10ng/ml bFGF 0.61 g/l Nicotinamide		Day 7-14: 20ng/ml OSM 50 mg/ml ITS$^+$ 1 μM Dexamethasone	HH Wu et al.
T3	Day 0-13 20ng/ml HGF 100 μM Dexamethasone 50 mg/ml ITS$^+$		Day 14-21: 20ng/ml OSM 100 mM Dexamethasone 50 mg/ml ITS$^+$	J Xin et al.
T4	Day 0-2: 10ng/ml FGF-4 1x ITS$^+$	Day 3-6: 20ng/ml HGF	Day 7-21: 20ng/ml HGF 1X ITS$^+$ 1 μg/ml Dexamethasone	S Snykers et al.
CTR	Control: 10% FBS	Control: 10% FBS	Control: 10% FBS	

FIG. 1. hBMSC differentiation protocols examined. *Top* is a diagram representing the duration and critical time point (*dashed lines*) during growth, differentiation, and maturation of a sequential differentiation program. Combo 1, 2, and 3 represent combinations of different growth factors, chemicals, and media additives based on specific protocols. *Bottom* table describes specific components and protocols for hBMSC differentiation. hBMSC, human bone marrow mesenchymal stromal cell.

ALB secretion and CYP450 activity assays

To confirm hepatic metabolic functions, hBMSCs were cultured on 96-well plates and CYP450 activity and ALB secretion were measured on day 21. Media were collected from 96-well plates and ALB secretion was evaluated using a quantitative human ALB enzyme-linked immunoassay kit (Fisher Scientific). A negative control (undifferentiated cells) and a positive control (primary hepatocytes) were similarly cultured. Three major cell-based human CYP450s were interrogated; the activities of CYP1A2, CYP3A4, and CYP2C9 were measured using the P450-Glo assay (Promega) following the manufacturer's instructions. CYP levels were measured 48 h after induction with 100 μM omeprazole for CYP1A2 and 25 μM rifampicin for CYP2C9 and CYP3A4.

Isolation and purification of total GAGs and compositional analysis

Both extracellular and intracellular GAG type and composition were measured throughout the differentiation protocol using previously described methodologies [15,17]. Briefly, cells were first washed with PBS and then incubated with 100 μL of BugBuster 10×Protein Extraction Reagent and sonicated for 1 h. Samples were desalted by passing through a 3 kDa molecular weight cutoff spin column and washed thrice with DDI water. The casing tubes were replaced before 300 μL of digestion buffer (50 mM ammonium acetate containing 2 mM calcium chloride adjusted to pH 7.0) was added to the filter unit. Recombinant heparin lyase I, II, and III and recombinant chondroitin lyase ABC (10 mU each) were added to each sample and mixed well. The samples were all placed in a 37°C incubator overnight, after which enzymatic digestion was terminated by removing the enzymes by centrifugation. The filter unit was washed twice with 300 μL DDI water and the filtrates containing the disaccharide products (molecular weight <700 Da) were dried by vacuum centrifugation. The dried samples were then treated with 10 μL of 0.1 M 2-aminoacridone (AMAC) in DMSO/acetic acid (17/3, v/v) at room temperature for 10 min, followed by adding 10 μL of 1 M aqueous sodium cyanoborohydride and incubating for 1 h at 45°C. A mixture containing all 17 disaccharide standards (Iduron) prepared at 0.5 ng/μL was similarly AMAC labeled and used for each run as an external standard.

After AMAC labeling, the samples were centrifuged and each supernatant was recovered. LC was performed on an Agilent 1200 LC system at 45°C using an Agilent Poroshell 120 ECC18 (2.7 μm, 3.0×50 mm) reverse phase column. Mobile phase A was 50 mM ammonium acetate aqueous solution and mobile phase B was methanol. The mobile phases

passed through the column at a flow rate of 300 μL/min. The gradient was 0–10 min, 5%–45% B; 10.0–10.2 min, 45%–100% B; 10.2–14.0 min, 100% B; and 14–22 min, 100%–5% B. The injection volume was 5 μL. A triple quadrupole mass spectrometry system equipped with an ESI source (Thermo Fisher Scientific, San Jose, CA) was used a detector. The online MS analysis was performed in the multiple reaction monitoring mode with negative ionization and a spray voltage of 3,000 V, a vaporizer temperature of 300°C, and a capillary temperature of 270°C.

Results from all experiments are expressed as mean ± standard deviation. Statistical analyses were performed using one-way analysis of variance and Student's *t*-test. The significance level was set at $P \leq 0.05$.

Results

Comparison of protocols for hBMSC differentiation toward human primary hepatocytes

The hBMSCs initially were evaluated for potential heterogeneity. To that end, flow cytometry was performed on the cell population and the major hBMSC markers, CD73, CD90, and CD105, were observed in >85%, 87%, and 60% of the total cells, respectively (Supplementary Fig. S1). This indicates that the starting cell population was highly homogenous for hBMSCs. Four culture protocols were examined to induce hepatic differentiation of hBMSCs isolated from fresh bone marrow at passages 3 or 4 (Fig. 1). These protocols were designed to induce differentiation through the EMT initiation stage with 20, 50, or 100 ng/mL of activin A (protocols T1A, B, and C respectively), or directly toward hepatocyte-like cells (protocols T2, T3, and T4). Under all these conditions, hBMSCs could differentiate toward hepatocyte-like cells. These cells showed a transition from the elongated spindle-like shape, typical of hMSCs, into varying morphologies (Fig. 2). Protocols T1A, B, and C yielded the fewest morphological changes toward the normal hepatic polygonal morphology (Fig. 2) [18,19]. With 25 ng/mL activin A (protocol T1A), only about 50% of the cells showed a more rounded morphology (Fig. 2; dashed circle), while the other 50% remained in a spindle-like shape (Fig. 2; arrow). Cells in both the T1B and C protocols remained spindle like, but much shorter. These morphological changes are consistent with previous reports on hBMSCs in the presence of EGF and FGF [20]. Protocol T2 showed the most homogeneous morphological transition into a polygonal shape. A heterogeneous population of mostly polygonal and a few spindle-like (arrow; Fig. 2) cells was observed in protocols T3 and T4.

Gene expression of the key hepatic markers, HNF-4α, AFP, and ALB, was quantified to determine whether these morphological changes are associated with changes at the transcriptional level. HNF-4α and AFP are distinct hepatic markers, with HNF-4α expressed at early stages of liver development and AFP activated due to liver injury [21,22]. ALB is a late hepatic marker and represents the functional state of induced hepatocyte-like cells.

On day 3, based on transcriptional increase from the undifferentiated hBMSC levels (Fig. 3), AFP levels were significantly higher compared with HNF-4α in protocols T1A and T3, while HNF-4α was significantly higher than AFP in protocol T4. ALB was expressed on day 3, and protocols T1A and T2 showed higher levels than with other protocols. By day 7, ALB levels dropped to almost zero and AFP expression also significantly decreased, while HNF-4α increased. As early-stage markers, HNF-4α and AFP showed a typical trend of early transition into the hepatic lineage with high transcription at early stages. By day 21, ALB and AFP showed a second upregulation event from the levels on day 7. AFP upregulation with protocol T2 on day 21 was highest among the four protocols. ALB upregulation in protocol T1A was significantly higher than protocols T1C, T2, and T4. However, even after 21 days of differentiation, ALB gene expression was significantly lower than

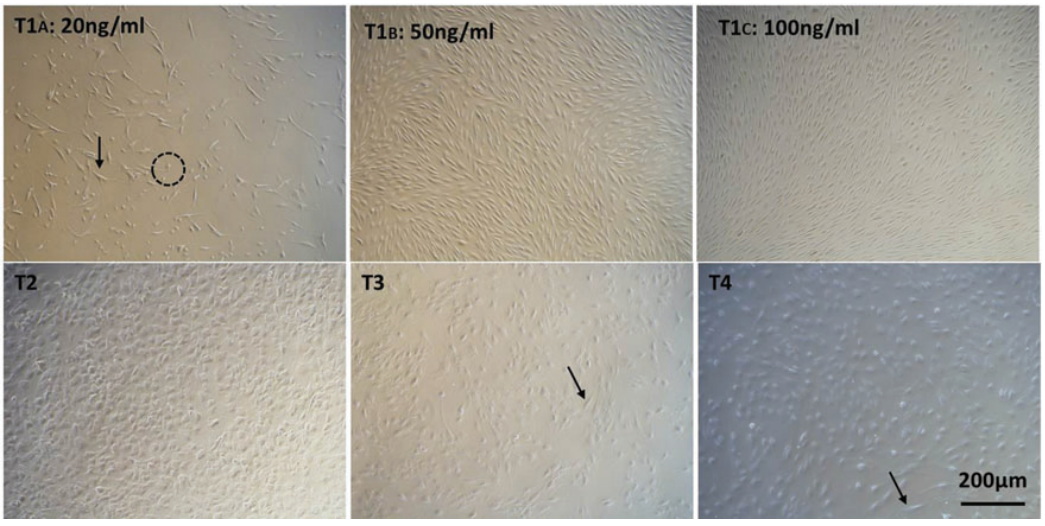

FIG. 2. Light microscopic analysis of hBMSC upon differentiation toward hepatocyte-like cells on day 21. *Arrows* indicate cells with spindle-like morphology. *Dashed circles* represent rounded morphology. 4× magnification (scale bar 200 μm). Color images are available online.

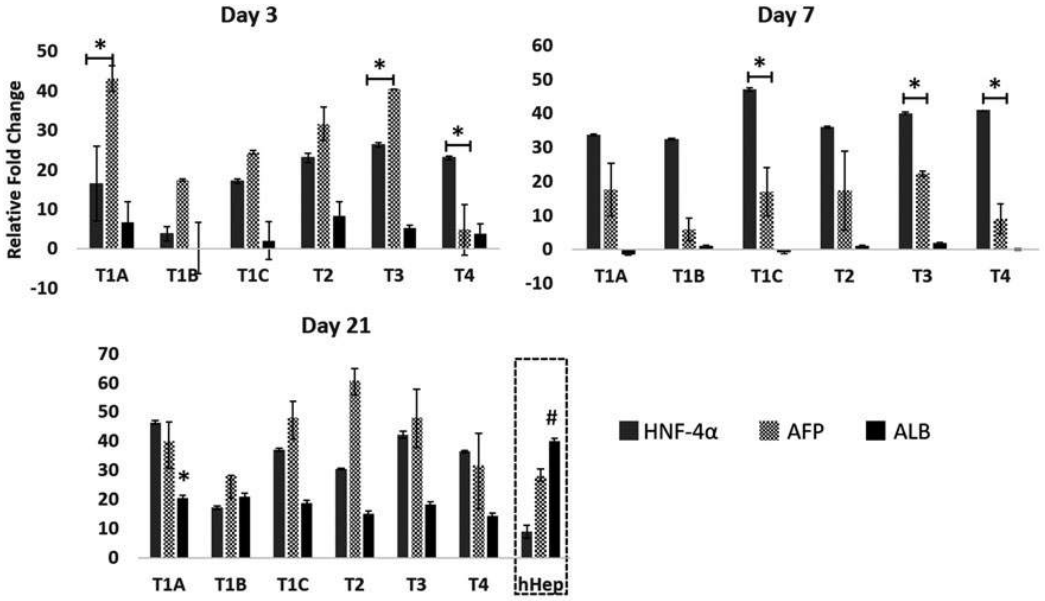

FIG. 3. Effect of differentiation protocols on key hepatic markers at different time points. Fold change in gene expression of ALB, AFP, and HNF was analyzed by qRT-PCR. The values of $2^{-\Delta\Delta CT}$ were calculated by normalizing to those of undifferentiated hBMSCs (CTR). The data are represented as averages ± SD, $n = 3$. ALB expression on day 21 was compared to that of human primary hepatocytes (*dashed box* at day 21). * and # indicate statistically significant changes of $P < 0.05$ and $P < 0.003$, respectively. AFP, α-fetoprotein; ALB, albumin; CTR, control; hHep, human hepatocytes; HNF, hepatocyte nuclear factor; qRT-PCR, real time-quantitative polymerase chain reaction; SD, standard deviation.

in primary hHEP, and AFP gene expression was high compared to primary hHEP. These results indicate a definitive transition toward hepatic lineage at the early stages and mid-stages of differentiation [20,22].

We next extended differentiation analysis to functional phenotypic properties of the differentiated hBMSCs. To that end, we examined ALB secretion, glycogen storage, and CYP450 isoform activity. ALB secretion is shown in Fig. 4, on day 21 of differentiation. All protocols showed significantly higher ALB levels than the undifferentiated hBMSCs control (CTR). Protocol T2 was significantly ($P < 0.05$) higher than protocols T1A, B, and C, and T3. The level of ALB in protocols T3 and T4 was also significantly higher than in protocols T1A and B. ALB secreted from primary hepatocytes was significantly higher compared with all differentiation protocols ($P < 0.05$), except for T2 ($P = 0.06$). This agrees with the gene expression data where ALB levels in differentiated hBMSCs were lower than in primary hepatocytes and confirms the mid-state differentiation of hBMSCs toward mature hepatocytes.

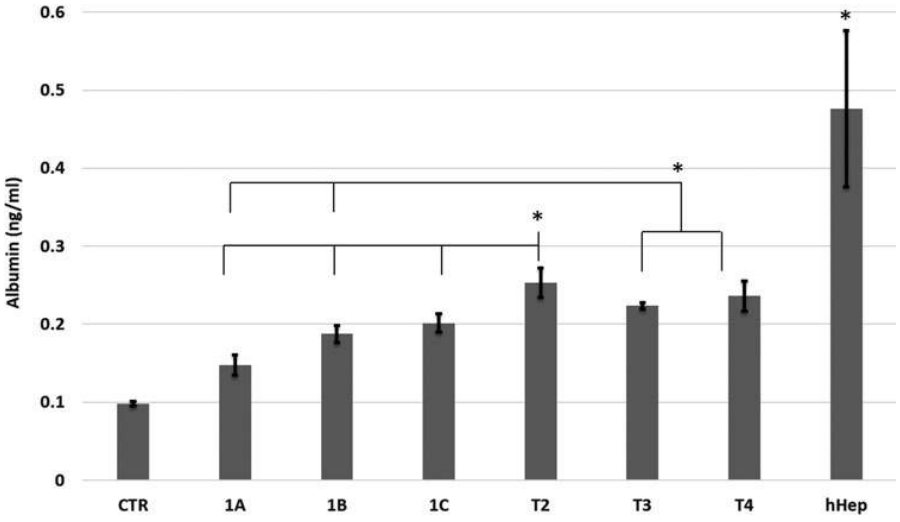

FIG. 4. ALB secretion at 21 days of differentiation. hBMSCs exposed to activin A resulted in significantly lower ALB levels than direct methods (protocols T2, T3, and T4). Data represented as average ± SD ($n = 3$). An *asterisk* (*) represents significance with $P < 0.05$.

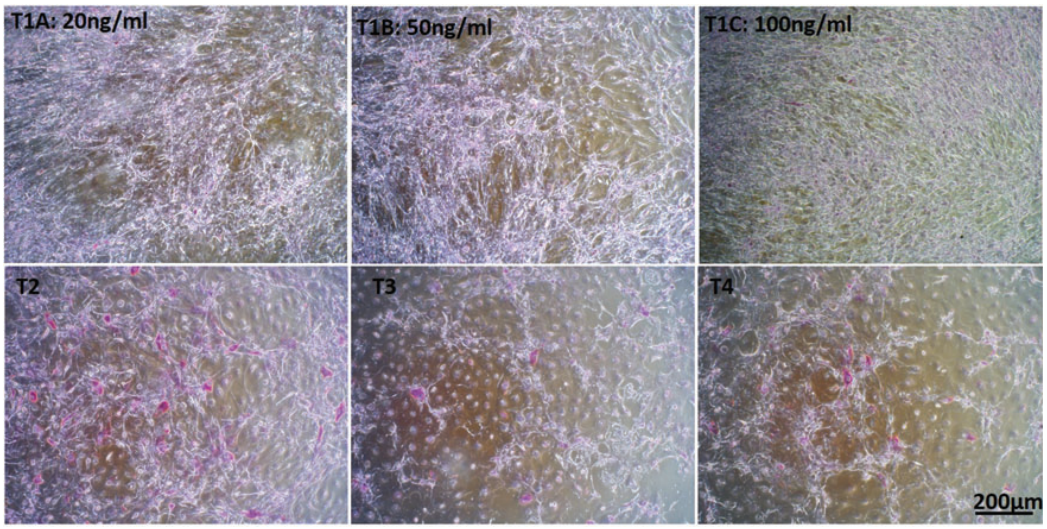

FIG. 5. Glycogen storage capacity of hBMSCs at 21 days of differentiation. *Top row*: hBMSCs exposed to 25, 50, and 100 ng/mL of activin A. *Bottom row*: hBMSCs directly differentiated toward hepatocytes without actvin A. Glycogen stains magenta color. Original magnification of 4×(scale bar 200 µm). Color images are available online.

PAS staining showed elevated accumulation of glycogen when hBMSCs were directly differentiated (protocols T2, T3, and T4) into hepatocyte-like cells (Fig. 5), in comparison to protocols T1A-C with a mesenchymal-to-epithelial (MET) initiation step. Protocol T2 showed higher glycogen accumulation when compared to protocols T3 and T4. With respect to CYP450 induction, we exposed differentiated hBMSCs and primary hepatocytes to 100 µM omeprazole to induce CYP1A2 activity and 25 µM rifampicin for CYP1A2 and CYP2C9 activity. As depicted in Fig. 6, as expected, CYP1A2, CYP2C9, and CYP3A4 were clearly induced in primary hHEP. In undifferentiated hBMSCs, very low activity of each CYP450 was observed. Differentiated hBMSCs showed significantly higher CYP450 activity over that of undifferentiated hBMSCs. However, CYP450 activity was several fold lower compared with primary hepatocytes, suggesting that fully mature hepatocytes were not formed after 21 days.

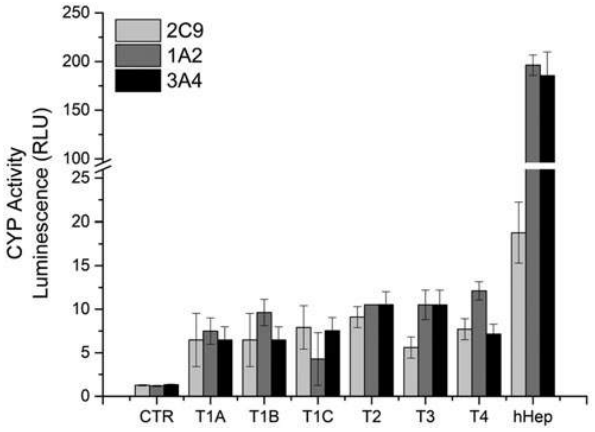

FIG. 6. Cytochromes P450 enzyme activity at 21 days of hBMSC differentiation. CYP450 activity was measured 48 h after induction with 100 µM omeprazole for CYP1A2 and 25 µM rifampicin for CYP2C9 and CYP3A4. Undifferentiated hBMSCs (CTR) represent the negative control and primary hHep represent the positive control. Data represented as average ± SD ($n = 3$).

Influence of differentiation on GAG content

Our overarching hypothesis is that different differentiation protocols will result in distinct GAG type and composition, and such differences can be used to optimize hBMSC differentiation into complex terminal cell types, including primary hepatocytes. To this end, we evaluated the GAG profiles of primary hepatocytes and differentiating hBMSCs using the various differentiation protocols as a function of time. Undifferentiated hBMSCs (CTR) on day 3 had higher levels of heparan sulfate (HS, 54% of total GAG content) and hyaluronic acid (HA, 32%) compared to chondroitin sulfate (CS, 14%) (Fig. 7). These values were relatively unaffected through day 21, indicating that the undifferentiated cells were stable for the duration of the experiment.

On day 3, the differentiating hBMSCs showed dramatically lower HS levels versus the undifferentiated cells, with the exception of protocol T4. The CS content remained roughly constant among the different protocols. Conversely, HA showed the opposite trend on day 3, and was significantly higher in the differentiating hBMScs than in undifferentiated cells, except for protocol T4. Extending differentiation to 7 days, HS content was significantly lower in protocols T1A and C and T2, when compared to the control. CS levels in protocol T2 were significantly lower than among the other protocols. HA significantly increased for protocols T1A and C and T2, and remained relatively the same for protocols T1B, T3, and T4, when compared to the undifferentiated hBMSCs. By day 21, a drop of HA levels in protocols T1A, B (significant), and C was observed, while

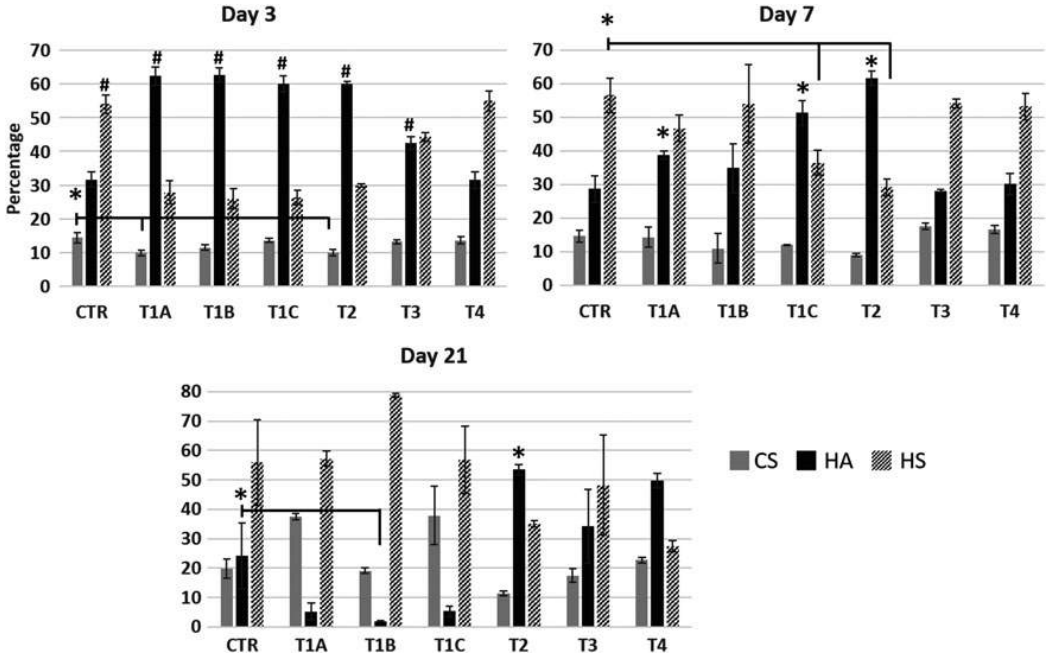

FIG. 7. LC-MS quantification of total glycosaminoglycans from cells collected on days 3, 7, and 21 of hBMSC differentiation. Changes are compared to undifferentiated hBMSCs (CTR) at each time point. Data presented as average ± SD ($n = 3$). * and # indicate statistically significant changes of $P < 0.05$ and $P < 0.003$, respectively. LC-MS, liquid chromatography–mass spectrometry.

an increase was obtained in protocols T2 (significant), T3, and T4, when compared to undifferentiated hBMSCs. An increase of HS levels was obtained in protocol T1B, while a drop in HS levels occurred in protocol T4. The GAG profile for primary hHEP was also examined and found to consist primarily of HS (95% of total GAG content) with HA and CS only 0.3% and 5%, respectively.

More detailed GAG compositional assessment can be made by evaluating the structure of the GAGs through disaccharide analysis. To this end, we digested HS and CS with heparinases and chondroitinase, respectively. For HS, these include *N*-acetylated HS chains (0S, 2S, 6S, and 2S6S) and *N*-sulfonated HS chains (NS, NS2S, and NS2S6S [or TriS]) as depicted in Fig. 8. For CS, these include *N*-acetylated CS chains (4S, 6S, 2S, 2S4S, 0S, 2S6S, and 4S6S) and *N*-sulfonated CS chains (TriS). The dominant HS structure consisted of the 0S (Fig. 9A); on day 3, 0S levels increased in protocols T1A and T4, and significantly increased in protocols T1B, T1C, and T2, while remained similar to undifferentiated hBMSCs in protocol T3. NS2S significantly decreased in protocol T1C on day 3, while slightly decreased in protocols T1A and B, and T2. NS significantly increased in protocol T1C compared to undifferentiated hBMSCs, and slightly decreased in all other protocols, with the exception of protocol T4. On day 7, a major transition in disaccharide composition was observed in protocol T1B, where a significant decrease in 0S (drop of 52%) was complemented by a significant increase in NS2S (3.6-fold) compared to undifferentiated hBMSCs. 0S was detected at higher levels in protocol T1A and at significantly higher levels in the other protocols when compared to the control. The day 3 trend for NS and NS2S levels in protocol T1C remained the same when compared to undifferentiated hBMSCs on day 7. After 21 days of differentiation, including maturation steps, the OS and NS2S disaccharide profiles did not change from day 7 for protocol T1B in comparison to undifferentiated hBMSCs. Although not significant, a drop in 0S and an increase in NS were observed in protocols T1C, T3, and T4 when compared to undifferentiated hBMSCs. All other disaccharide (2S, 6S, 2S6S, NS6S, and TriS) levels (the sum of the averages is shown) were negligible (<6% on day 3, < 8% on day 7, and <12% on day 21). Of the HS present in human primary hepatocytes (~95% of total GAG), 68% 0S, 24% NS, and 9% of the other disaccharides were detected (data not shown). When compared to primary hHEP, the best performing protocol, T2, only expressed ~35% HS as a function of total GAG on day 21, of which 60% consisted of 0S and 21% NS. Although the individual disaccharide profiles are close to that of human primary hepatocytes, the total HS detected is 2.7-fold lower in protocol T2. For protocol T1B, the GAG HS content was 79% on day 21, and of that, less than one-quarter was 0S and two-thirds was NS2S.

This comparison highlights the impact of understanding and tracking GAG changes and GAG structure, as reflected in disaccharide profiles during differentiation. Cytokines and chemical additives clearly influence the newly forming ECM. For example, bEGF and FGF are shown to prime hBMSCs for hepatic differentiation, while nicotinamide (protocols T1A-C in the differentiation step) and dexamethasone (all protocols at the maturation step) are known

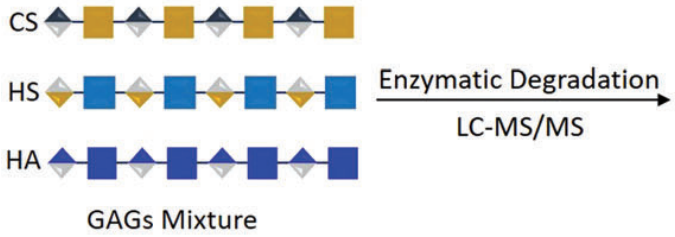

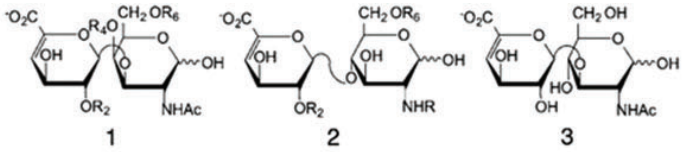

CS disaccharides	structure 1	R_2	R_4	R_6
$TriS_{CS}$	ΔUA2S(1,3)GalNAc4S6S	SO_3^-	SO_3^-	SO_3^-
$2S4S_{CS}$	ΔUA2S(1,3)GalNAc4S	SO_3^-	SO_3^-	H
$2S6S_{CS}$	ΔUA2S(1,3)GalNAc6S	SO_3^-	H	SO_3^-
$4S6S_{CS}$	ΔUA(1,3)GalNAc4S6S	H	SO_3^-	SO_3^-
$2S_{CS}$	ΔUA2S(1,3)GalNAc	SO_3^-	H	H
$4S_{CS}$	ΔUA(1,3)GalNAc4S	H	SO_3^-	H
$6S_{CS}$	ΔUA(1,3)GalNAc6S	H	H	SO_3^-
$0S_{CS}$	ΔUA(1,3)GalNAc	H	H	H
HS disaccharides	**structure 2**	R_2	NR	R_6
$TriS_{HS}$	ΔUA2S(1,4)GlcNS6S	SO_3^-	SO_3^-	SO_3^-
$NS6S_{HS}$	ΔUA(1,4)GlcNS6S	H	SO_3^-	SO_3^-
$NS2S_{HS}$	ΔUA2S(1,4)GlcNS	SO_3^-	SO_3^-	H
NS_{HS}	ΔUA(1,4)GlcNS	H	SO_3^-	H
$2S6S_{HS}$	ΔUA2S(1,4)GlcNAc6S	SO_3^-	Ac	SO_3^-
$6S_{HS}$	ΔUA(1,4)GlcNAc6S	H	Ac	SO_3^-
$2S_{HS}$	ΔUA2S(1,4)GlcNAc	SO_3^-	Ac	H
$0S_{HS}$	ΔUA(1,4)GlcNAc	H	Ac	H
HA disaccharides	**structure 3**			
$0S_{HA}$	ΔUA(1,3)GlcNAc			

FIG. 8. Schematic depiction of the various HS and CS disaccharides. CS, chondroitin sulfate; HS, heparan sulfate. Color images are available online.

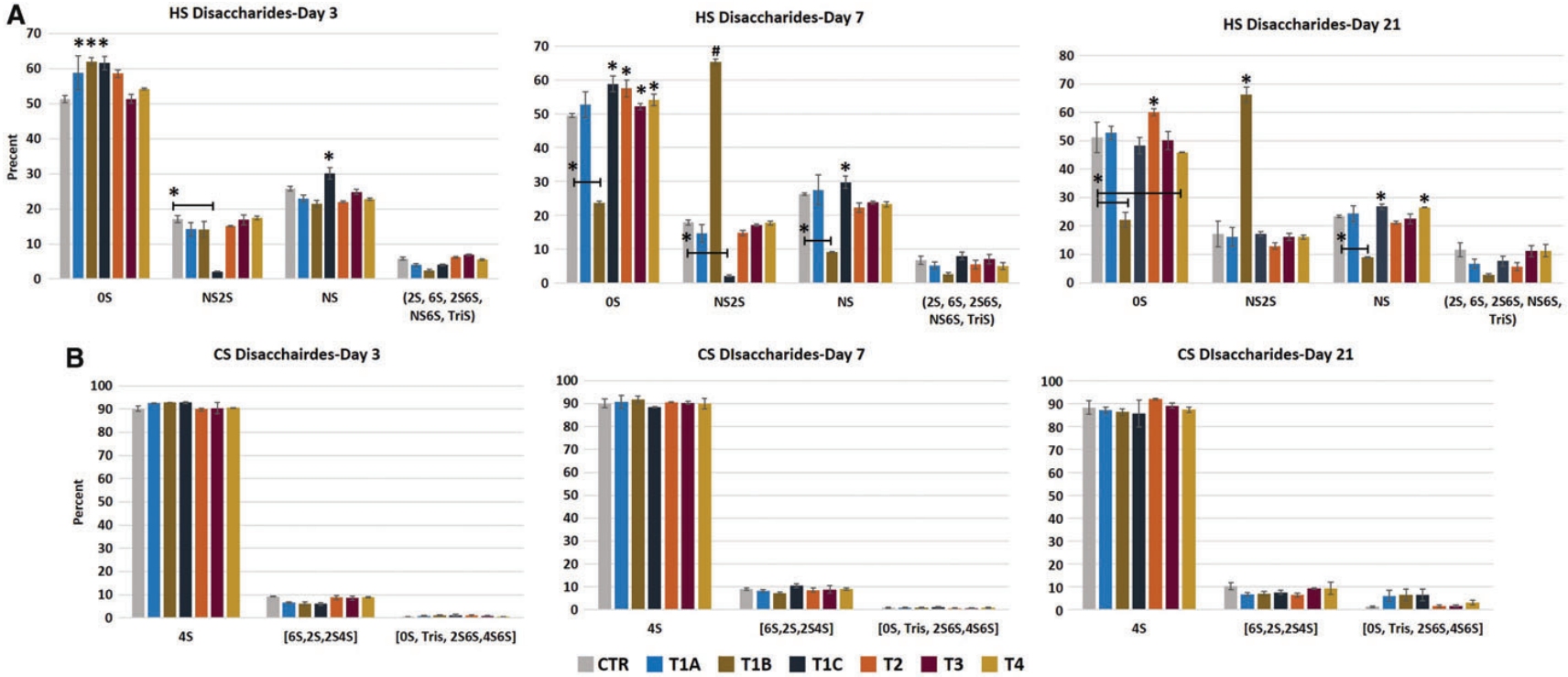

FIG. 9. LC-MS analysis of percent abundance of individual disaccharides from cells collected on days 3, 7, and 21 of hBMSC differentiation. **(A)** HS and **(B)** CS. Data are compared to the undifferentiated hBMSCs (CTR) at each time point. Data presented as average ± SD ($n = 3$). * and # indicate statistically significant changes of $P < 0.05$ and $P < 0.003$, respectively. Color images are available online.

to be potent differentiation inducers [20,23]. However, in the case of T1A-C, the addition of activin A for 24 h was not sufficient to fully induce MET transition. Thus, if bEGF and FGF are primers for BMSCs into hepatic lineage, the addition of activin A at early stage was not adequate or even needed. The GAG profile of protocols T1A-C is slightly more consistent throughout 21 days of differentiation, but the disaccharide profile does not match that of primary hHEP. In the case of protocol T2, the differentiation was more successful and the disaccharide profile for HS was relatively similar to that of primary hHEP (Fig. 9A).

The disaccharide profile for CS (Fig. 9B) revealed 4S to be the dominant disaccharide in all protocols and its level was maintained throughout 21 days of differentiation. The combined averages for 6S, 2S, and 2S4S and the combined averages for 0S, 2S6S, 4S6S, and TriS also remained relatively constant. Disaccharide analysis of primary hHEP (not shown) revealed that of the 0.3% CS detected, 4S (64%) and 0S (26%) were the dominant disaccharides. The CS profile in general is similar to that of the undifferentiated hBMSCs throughout 21 days of differentiation, another indication of lack of functional maturity.

Discussion

BMSCs are an ideal autogenetic and allogenic multipotent source of stem cells for the repair and regeneration of tissues and organs. hBMSCs are readily available and methods of isolation are straightforward. Indeed, clinical approaches have been developed to concentrate bone marrow (Magellan® System; Arteriocyte Medical Systems) for therapeutic use, for example, autologous chondrocyte implantation [24–26]. BMSCs have the innate machinery for homing and release of trophic mediators [27–29]. BMSCs also have immunomodulatory capability, and thus avoid an immune response [30]. Mesenchymal stromal cells have been shown to differentiate into hepatic-like cells. However, the methods used have varied in terms of species (human, mouse, and rat), cell source (bone marrow, umbilical cord, and adipose tissue), and differentiation protocols (sequential vs. cocktail).

To assess differentiation and maturation, many methods have been used such as imaging, gene and protein expression, and immunohistochemistry. In this study, we implemented multiple protocols and assessed their success based on a combination of established methods, including cell morphology, gene expression, glycogen storage, ALB secretion, and CYP450 activity. Lee et al. (protocols T1A-C) examined the potential of human adipose stem cells isolated from abdominal fat tissue as a source of personalized therapy for liver failure [31]. The authors concluded that early differentiation and maturation depended on the concentration of activin A. With higher activin A concentration, early differentiation was observed and cells exhibited hepatocyte-like shape. Activin A is a member of the transforming growth factor beta 1 (TGF-β) superfamily and is involved in the activation of the Wnt/β-catenin pathway. Since hepatocytes are from the endoderm lineage, it is believed that MET is necessary for MSCs to differentiate into hepatocytes [32–34]. This is contrary to our study, where we found cells begin to shrink, but maintain their spindle-like morphology even on day 21 (after step 3). This transition is less uniform at lower activin A concentrations. Gene expression data contradict the study by Lee et al. AFP increased with 100 ng/mL activin A by day 21 and was higher than at 20 or 50 ng/mL. HNF-4α decreased on day 21 for 50 and 100 ng/mL of activin A and increased for 20 ng/mL, which is in agreement with Lee et al. ALB gene expression increased on day 21 for all concentrations of activin A, and lower concentrations showed significantly higher ALB similar to Lee et al.

Other researchers have successfully differentiated MSCs into hepatocytes like using a combination of factors, including HGF, EGF, βFGF, dexamethasone, DMSO, and nicotinamide without activin A [9,35–37]. However, the challenge in potentially using hBMSCs in vitro and especially in vivo is the lack of achieving terminally differentiated cells that maintain functionality for long periods. Additional studies, therefore, are necessary to understand the influence of the local microenvironment and to elucidate further the effects of cytokines and chemical compounds. The role of ECM proteins and GAGs on cellular behavior is well established, although the majority of studies have examined the naive and final stages of a differentiation. To the best of our knowledge, our study is the first to examine the temporal evolution of major GAGs and their constituent disaccharides on stromal and other stem-like cells during differentiating.

In this study, protocol T2 performed better than protocols T3 and T4, and significantly better than protocols T1A-C, based on morphological transition into polygonal cells, glycogen storage, and ALB secretion. Protocol T2 was adapted from Wu et al. [37], where BMSCs were isolated from 7- to 8-week-old Balb/c mice. Our results are similar to Wu et al. in that on day 21, cells had hepatocyte-like morphology, although the transition was much more uniform and more robust than protocols adopted from Xin et al. (protocol T3) and Snykers et al. (T4). ALB secretion and glycogen storage in protocol T2 were higher than in protocols T3 and T4. Although Xin et al. used hBMSCs, the bone marrow mixture was collected from four different donors, whereas our cells were collected from a single donor [36]. This could result in interindividual variability for which we did not account. Although ALB levels were lower than in primary hHEP, such levels were in agreement with reported levels for differentiated adult stem or stromal cells [31,35]. In all protocols, CYP450 activity was significantly higher than in undifferentiated hBMSCs, although they remained far lower than CYP450 activity in primary hHEP. In aggregate, these results strongly suggest that the differentiated cells represent early-/mid-stage hepatic lineage and further maturation is required. To the best of our knowledge, this is the first time CYP450 activity and ALB secretion of hepatocyte-like cells from hBMSCs have been compared to primary hHEP.

To gain greater insight into the effect of various differentiation protocols on cell fate (eg, differentiation state, cell morphology, gene expression, and protein expression), we addressed the GAG profile as a function of differentiation protocols. Specifically, GAG remodeling was examined with respect to major GAGs and their structures (eg, disaccharide composition), for use as a ''marker'' to evaluate the progress of hBMSC differentiation. The parental hBMSC population was HS rich and maintained its GAG composition over the 21 days of culturing, indicating the stable nature of primary adult hBMSCs. By day 7, protocols T1A, B, T3, and T4 yielded cells that reverted to an HS-rich GAG profile. On day 21, HA levels in protocols T1A, B, and

C had significantly dropped versus undifferentiated hBMSCs and versus differentiated cells on day 7.

Li et al. showed that activin A has specific binding affinity to HS [38]. This could explain why higher concentrations in protocol T1C showed better performance than lower concentrations (protocols T1A and B). HS levels are high in undifferentiated hBMSCs, and since activin A was added for only 1 day during early differentiation stages, the higher concentration may have significantly influenced cell fate. Similar to activin A, HGF has high affinity to HS and is involved in cell proliferation, morphogenesis, and wound healing [39]. HGF also has high affinity to MET factor (Met), a tyrosine kinase receptor. HS also mediates this interaction. This unique HGF-Met complex formation activates Met, which in turn allows for diverse biological responses of HGF [40–43]. This could explain the superior effect of HGF to activin A. During the T2 differentiation protocol, HGF was maintained in the culture medium for up to 6 days, while in protocol T3, it was added for 13 days. The longer exposure of HGF did not support further differentiation of hBMSCs to hepatocytes, perhaps due to significant reduction of HS levels by day 7, which can, in part, be due to lack of cellular priming at early differentiation stages. While in protocol T4, HGF was not introduced until day 3, at which point HS had decreased. Thus, the initial amount and duration of use of growth factor based on HS profile played a significant role in hBMSC differentiation.

Looking closer at protocol T2, cells are primed with bFGF, but these cells are also exposed to two powerful, yet conflicting signaling agents. HGF is a potent mitogenic and proliferative cytokine, and is involved in both endoderm development and liver regeneration. However, nicotinamide is a strong differentiation agent, and thus, its addition at a very early stage might negatively affect cellular progression into fully functional hepatocytes. Sequential addition of cytokines and other compounds are known to be far more potent than cocktail-based protocols [9]. Thus, perhaps a two-stage protocol (T2) is not sufficient. From the combined results presented in this study, a four-stage protocol is proposed. Stage one begins with priming by the addition of EGF and/or bFGF. A second stage would involve the addition of a hepatic inducer such as HGF or FGF-4 with or without priming agents. The third stage then would be HGF with either a combination of dexamethasone and nicotinamide or each alone. Finally, a fourth stage would be the maturation with a combination of dexamethasone and nicotinamide or each alone. GAGs and their perspective disaccharide profiles would be examined to determine the optimal conditions.

In summary, these results demonstrate the effect of GAG remodeling on hBMSC fate. We hypothesize that by controlling the GAG profile, it may be possible to advance hBMSC differentiation toward primary hHEP. Such control can be achieved by careful choice of cell culture medium composition and treatment protocols in a 3D environment. These results lay the groundwork for future in vivo studies on the role of GAGs in hBMSC differentiation to hepatocytes.

Acknowledgments

This study was supported by the National Institutes of Health (grant no. ES020903), Taconic Biosciences, Inc., and the Heparin Applied Research Center.

Author Disclosure Statement

No competing financial interests exist.

Supplementary Material

Supplementary Figure1

References

1. Ye JS, XS Su, J-F Stoltz, N de Isla and L Zhang. (2015). Signalling pathways involved in the process of mesenchymal stem cells differentiating into hepatocytes. Cell Prolif 48:157–165.
2. Best J, P Manka, W-K Syn, L Dollé, LA van Grunsven and A Canbay. (2015). Role of liver progenitors in liver regeneration. Hepatobiliary Surg Nutr 4:48–58.
3. Zhang Z, J Liu, Y Liu, Z Li, WQ Gao and Z He. (2013). Generation, characterization and potential therapeutic applications of mature and functional hepatocytes from stem cells. J Cell Physiol 228:298–305.
4. Li Q, AP Hutchins, Y Chen, S Li, Y Shan, B Liao, D Zheng, X Shi, Y Li, et al. (2017). A sequential EMT-MET mechanism drives the differentiation of human embryonic stem cells towards hepatocytes. Nat Commun 8:1–12.
5. Godoy P, W Schmidt-Heck, K Natarajan, B Lucendo-Villarin, D Szkolnicka, A Asplund, P Björquist, A Widera, R Stöber, et al. (2015). Gene networks and transcription factor motifs defining the differentiation of stem cells into hepatocyte-like cells. J Hepatol 64:525–526.
6. Lo B and L Parham. (2009). Ethical issues in stem cell research. Endocr Rev 30:204–213.
7. Kajiwara M, T Aoi, K Okita, R Takahashi, H Inoue, N Takayama, H Endo, K Eto, J Toguchida, S Uemoto and S Yamanaka. (2012). Donor-dependent variations in hepatic differentiation from human-induced pluripotent stem cells. Proc Natl Acad Sci U S A 109:12538–12543.
8. Teng N-Y, Y-S Liu, H-H Wu, Y-A Liu, JH Ho and OK-S Lee. (2015). Promotion of mesenchymal-to-epithelial transition by Rac1 inhibition with small molecules accelerates hepatic differentiation of mesenchymal stromal cells. Tissue Eng Part A 21:1444–1454.
9. Snykers S, T Vanhaecke, P Papeleu, A Luttun, Y Jiang, Y Vander Heyden, C Verfaillie and V Rogiers. (2006). Sequential exposure to cytokines reflecting embryogenesis: the key for in vitro differentiation of adult bone marrow stem cells into functional hepatocyte-like cells. Toxicol Sci 94:330–341.
10. Roelandt P, P Sancho-Bru, K Pauwelyn and C Verfaillie. (2010). Differentiation of rat multipotent adult progenitor cells to functional hepatocyte-like cells by mimicking embryonic liver development. Nat Protoc 5:1324–1336.
11. Ahn SH, HJ Lee, JS Lee, H Yoon, W Chun and GH Kim. (2015). A novel cell-printing method and its application to hepatogenic differentiation of human adipose stem cell-embedded mesh structures. Sci Rep 5:1–11.
12. Meli L, ET Jordan, DS Clark, RJ Linhardt and JS Dordick. (2012). Influence of a three-dimensional, microarray environment on human cell culture in drug screening systems. Biomaterials 33:9087–9096.
13. Suzuki A. (2003). Role for growth factors and extracellular matrix in controlling differentiation of prospectively isolated hepatic stem cells. Development 130:2513–2524.
14. Ragelle H, A Naba, BL Larson, F Zhou, M Prijić, CA Whittaker, A Del Rosario, R Langer, RO Hynes and DG Anderson. (2017). Comprehensive proteomic characterization

of stem cell-derived extracellular matrices. Biomaterials 128: 147–159.
15. Gasimli L, AM Hickey, B Yang, G Li, MD Rosa, AV Nairn, MJ Kulik, JS Dordick, KW Moremen, S Dalton and RJ Linhardt. (2014). Changes in glycosaminoglycan structure on differentiation of human embryonic stem cells towards mesoderm and endoderm lineages. Biochim Biophys Acta Gen Subj 1840:1993–2003.
16. Li G, L Li, F Tian, L Zhang, C Xue and RJ Linhardt. (2015). Glycosaminoglycanomics of cultured cells using a rapid and sensitive LC-MS/MS approach. ACS Chem Biol 10:1303–1310.
17. Li B, H Liu, Z Zhang, HE Stansfield, JS Dordick and RJ Linhardt. (2011). Analysis of glycosaminoglycans in stem cell glycomics. Methods Mol Biol 690:285–300.
18. Arterburn LM, J Zurlo, JD Yager, RM Overton and AH Heifetz. (1995). A morphological study of differentiated hepatocytes in vitro. Hepatology 22:175–187.
19. Zhang R, T Takebe, K Sekine, H Koike, Y Zheng and H Taniguchi. (2014). Identification of proliferating human hepatic cells from human induced pluripotent stem cells. Transplant Proc 46:1201–1204.
20. Chivu M, SO Dima, CI Stancu, C Dobrea, V Uscatescu, LG Necula, C Bleotu, C Tanase, R Albulescu, C Ardeleanu and I Popescu. (2009). In vitro hepatic differentiation of human bone marrow mesenchymal stem cells under differential exposure to liver-specific factors. Transl Res 154:122–132.
21. Hayhurst GP, Y-H Lee, G Lambert, JM Ward and FJ Gonzalez. (2001). Hepatocyte nuclear factor 4α (nuclear receptor 2A1) is essential for maintenance of hepatic gene expression and lipid homeostasis. Mol Cell Biol 21:1393–1403.
22. Wederell ED, M Bilenky, R Cullum, N Thiessen, M Dagpinar, A Delaney, R Varhol, Y Zhao, T Zeng, et al. (2008). Global analysis of in vivo Foxa2-binding sites in mouse adult liver using massively parallel sequencing. Nucleic Acids Res 36:4549–4564.
23. Liu M and Y Wang. (2014). Mechanism of MSCs differentiation into hepatocyte-like cells: the role of cytokines and chemical compounds. J Stem Cell Res Ther 4:179.
24. Brittberg M, A Lindahl, A Nilsson, C Ohlsson, O Isaksson and L Peterson. (1994). Treatment of deep cartilage defects in the knee with autologous chondrocyte transplantation. N Engl J Med 331:889–895.
25. Gobbi A, E Kon, M Berruto, G Filardo, M Delcogliano, L Boldrini, L Bathan and M Marcacci. (2009). Patellofemoral full-thickness chondral defects treated with second-generation autologous chondrocyte implantation: results at 5 years' follow-up. Am J Sport Med 37:1083–1092.
26. Mikael PE, X Xin, M Urso, X Jiang, L Wang, B Barnes, AC Lichtler, DW Rowe and SP Nukavarapu. (2014). A potential translational approach for bone tissue engineering through endochondral ossification. Conf Proc IEEE Eng Med Biol 2104:3925–3928.
27. Caplan AI and D Correa. (2011). The MSC: an injury drugstore. Cell Stem Cell 9:11–15.
28. Caplan AI and JE Dennis. (2006). Mesenchymal stem cells as trophic mediators. J Cell Biochem 98:1076–1084.
29. da Silva Meirelles L, AM Fontes, DT Covas and AI Caplan. (2009). Mechanisms involved in the therapeutic properties of mesenchymal stem cells. Cytokine Growth Factor Rev 20:419–427.
30. Caplan AI and JM Sorrell. (2015). The MSC curtain that stops the immune system. Immunol Lett 168:136–139.
31. Lee SW, SO Min, SY Bak, HK Hwang and KS Kim. (2015). Efficient endodermal induction of human adipose stem cells using various concentrations of Activin A for hepatic differentiation. Biochem Biophys Res Commun 464:1178–1184.
32. Vasconcellos R, ÉC Alvarenga, RC Parreira, SS Lima and RR Resende. (2016). Exploring the cell signalling in hepatocyte differentiation. Cell Signal 28:1773–1788.
33. Li J, L Zhu, X Qu, J Li, R Lin, L Liao, J Wang, S Wang, Q Xu and RC Zhao. (2013). Stepwise differentiation of human adipose-derived mesenchymal stem cells toward definitive endoderm and pancreatic progenitor cells by mimicking pancreatic development in vivo. Stem Cells Dev 22:1576–1587.
34. Shen MM. (2007). Nodal signaling: developmental roles and regulation. Development 134:1023–1034.
35. Li J, R Tao, W Wu, H Cao, J Xin, J Guo, L Jiang, X Hong, AA Demetriou, D Farkas and L Li. (2010). Transcriptional profiling and hepatogenic potential of acute hepatic failure-derived bone marrow mesenchymal stem cells. Differentiation 80:166–174.
36. Xin J, W Ding, S Hao, L Jiang, Q Zhou, T Wu, D Shi, H Cao, L Li and J Li. (2015). Human bone marrow mesenchymal stem cell-derived hepatocytes express tissue inhibitor of metalloproteinases 4 and follistatin. Liver Int 35:2301–2310.
37. Wu HH, JH Ho and OK Lee. (2016). Detection of hepatic maturation by Raman spectroscopy in mesenchymal stromal cells undergoing hepatic differentiation. Stem Cell Res Ther 7:1–10.
38. Li S, C Shimono, N Norioka, I Nakano, T Okubo, Y Yagi, M Hayashi, Y Sato, H Fujisaki, et al. (2010). Activin A binds to perlecan through its pro-region that has heparin/heparan sulfate binding activity. J Biol Chem 285:36645–36655.
39. Matsumoto K and T Nakamura. (2001). Hepatocyte growth factor: renotropic role and potential therapeutics for renal diseases. Kidney Int 59:2023–2038.
40. Catlow KR, JA Deakin, Z Wei, M Delehedde, DG Fernig, E Gherardi, JT Gallagher, MSG Pavão and M Lyon. (2008). Interactions of hepatocyte growth factor/scatter factor with various glycosaminoglycans reveal an important interplay between the presence of iduronate and sulfate density. J Biol Chem 283:5235–5248.
41. Deakin JA, BS Blaum, JT Gallagher, D Uhrín and M Lyon. (2009). The binding properties of minimal oligosaccharides reveal a common heparan sulfate/dermatan sulfate-binding site in hepatocyte growth factor/scatter factor that can accommodate a wide variety of sulfation patterns. J Biol Chem 284:6311–6321.
42. Kim ES and R Salgia. (2009). MET pathway as a therapeutic target. J Thorac Oncol 4:444–447.
43. Lindsey S and SA Langhans. (2015). Epidermal growth factor signaling in transformed cells. Int Rev Cell Mol Biol 314:1–41.

Address correspondence to:
Prof. Jonathan S. Dordick
Department of Chemical and Biological Engineering
Rensselaer Polytechnic Institute
110, 8th Street, 4005 CBIS
Troy, NY 12180-3522

E-mail: dordick@rpi.edu

Received for publication September 17, 2018
Accepted after revision December 12, 2018
Prepublished on Liebert Instant Online December 20, 2018